

## VERTICAL DISCRETIZATION AND COORDINATE SYSTEMS

Fedor Mesinger

UCAR Visiting Research Program, National Meteorological Center,  
Washington D.C.

Summary: Topics related to vertical discretization which have received attention up to the time of several years ago and which are covered by the existing review papers will be listed and briefly summarized. Following this introduction more recent work as well as work in progress will be reviewed and/or pointed out. Issues addressed will be those of the vertical discretization techniques, of the vertical resolution, and of the vertical coordinate systems. This will include an examination of the impact of the step-mountain ( $\eta$ ) compared to the terrain-following ( $\sigma$ ) vertical coordinate in a set of three forecasts done with one and then the other of these two systems but with no other differences in the model. In this set of three forecasts a benefit from using the step-mountain coordinate is demonstrated.

### 1. INTRODUCTION

Quite a variety of issues has been looked into dealing specifically with the vertical discretization of the atmospheric equations of motion. There exists a large body of review articles in which many of these issues are discussed. The previous ECMWF seminar on numerical methods, in 1983, has covered some of them (ECMWF, 1984). The latest review article with extensive coverage of a number of vertical discretization topics is probably the one by Arakawa (1988). I shall use it here for a brief run-down of major topics and as reference in summarizing the understanding of the issues involved as of several years ago.

Choice of the vertical coordinate is typically the first vertical discretization topic discussed. Geometric height, pressure, pressure normalized by surface pressure (" $\sigma$ "), potential temperature, and various generalizations and combinations of those have all been or are being used. Arakawa provides an extensive list of benefits and disadvantages of these choices as seen from a number of points of view. It is an issue attracting increasing interest in recent years and one which I will cover in more detail later on in this lecture.

Formulation of the lower and particularly the upper boundary condition is another important vertical discretization topic. Spurious energy reflection due to the artificial top boundary condition is a matter of concern. At this seminar a separate lecture will be devoted to this topic however.

Distribution of dependent variables in the vertical is one more topic which can be considered from a number of points of view. Arakawa (1988) reviews the work of Tokioka (1978) in which wave propagation and computational mode characteristics were studied regarding their dependence on the choice of the vertical grid. Arakawa has added examples of the amplitude of the computational mode for two vertical resolutions and for three choices of the vertical distribution of layer thickness. His examples demonstrate the aggravation of the computational mode problem with an increase in the vertical resolution. Arakawa attributes the computational mode to the definition of temperature and horizontal velocities at the same levels ("the Lorenz grid") used in the examples he showed. This unstaggered distribution is associated with an extra degree of freedom with respect to the thermal wind balance.

The reason why the Lorenz grid is still popular is the ease of the construction of schemes having various conservation properties. A very general analysis of a technique which can be used to impose conservation of a chosen function of the vertically advected variable can be found in Arakawa and Lamb (1977).

One more topic Arakawa (1988) reviews at some length is that of the false short-wave baroclinic instability due to the extra degree of freedom of the Lorenz grid pointed out above. The "Charney-Phillips grid", with temperatures defined between the horizontal velocity components, does not suffer from the problem (Arakawa and Moorthi, 1988).

In the continuation of this lecture I will cover three vertical discretization areas which have more recently been receiving a fair amount of attention: the vertical discretization techniques, the vertical resolution requirements, and the choice of the vertical coordinate.

## 2. DISCRETIZATION TECHNIQUES

Essentials of discretization techniques have already been covered by several preceding lectures at this seminar. A variety of approaches has been presented.

Choices are no less abundant when it comes to specific application to the vertical dimension in atmospheric models. Various finite-difference (or, "grid point", see Cullen, these proceedings, allowing for a separate definition of "finite-volume"), finite-element (e.g., Steppeler, 1989), and spectral techniques have all been and are being used. I will here restrict myself to just two examples in order to illustrate the wide divergence in the basic approaches to the problem.

One is a very recent study of Leslie and Purser (1991b; also Purser and Leslie, 1991). First, they compare the performance of various vertical staggering of variables in terms of the reproduction of the vertical modes of the governing equations linearized for a given basic state atmosphere. The vertical staggarings Leslie and Purser consider are those of Lorenz and Charney-Phillips referred to above, with three versions of the location of diagnostic

variables (geopotential and vertical velocity) for the Lorenz grid. They evaluate the performance of these vertical "grids" for 2nd, 4th and 6th-order numerical schemes based on Lagrange polynomials, and for a 6th-order "compact" scheme. With their Lagrange polynomials scheme, Leslie and Purser compute geopotential as well as vertical velocities by vertical integration of the Lagrange interpolation formula used for temperature and for horizontal mass divergence, respectively (Leslie and Purser, 1991a). For an assessment of accuracy Leslie and Purser examine the relative equivalent depth, the numerical value divided by the true value of the equivalent depth. For the lower modes, they find the depth error decreasing with the order of accuracy, and the 6th-order compact scheme significantly outperforming the corresponding Lagrange scheme. For the higher modes, only the Charney-Phillips grid resulted in a relative equivalent depth close to unity thereby avoiding the problem of anomalously small equivalent depths for the highest modes of their three schemes on the Lorenz grid.

Leslie and Purser (1991b) have also made forecast experiments in which they compare the performance of 15-level model runs with four of their vertical schemes against a "control" 31-level version of the same model. The model used was the current Bureau of Meteorology Research Centre (BMRC) operational model (Leslie et al., 1985). Comparisons were made in terms of root-mean-square (rms) differences ("errors") in wind and geopotential height. For a sample of 100 24-h forecasts, differences were clearly decreasing with increasing order of accuracy, and, for the two 6th-order schemes, when replacing the Lagrange by the compact scheme. Leslie and Purser also show an example of one of their forecasts in which the compact scheme has led to a marked improvement over the 2nd order scheme in terms of the location and depth of a cyclone center over Australia. Except for the compact scheme, Leslie and Purser present similar rms error and test forecast results in their earlier paper (1991a) referred to above.

Results of Leslie and Purser are in striking contrast with the approach emphasizing the conservation of various integral quantities in vertical discretization introduced by Arakawa (e.g., Arakawa and Lamb, 1977). Using the Lorenz grid with layer values having integer indices and interface values having "half" indices, respectively, (Fig. 1) Arakawa and Lamb discretize the vertical advection of a variable A carried at layers ("full levels") as

$$\left(\dot{\sigma} \frac{\partial A}{\partial \sigma}\right)_L = \frac{1}{\Delta \sigma_L} \left(\dot{\sigma}_{L+1/2} (\hat{A}_{L+1/2} - A_L) + \dot{\sigma}_{L-1/2} (A_L - \hat{A}_{L-1/2})\right) \quad (1)$$

with the interface value of A, denoted  $\hat{A}$ , yet to be determined. Arakawa and Lamb see this as a possible means of satisfying an integral constraint in addition to the constraint of conserving the difference analog of the global integral of A with respect to mass which (1) already satisfies. They demonstrate that a difference analog of the global integral of F(A) with respect to mass will be conserved if

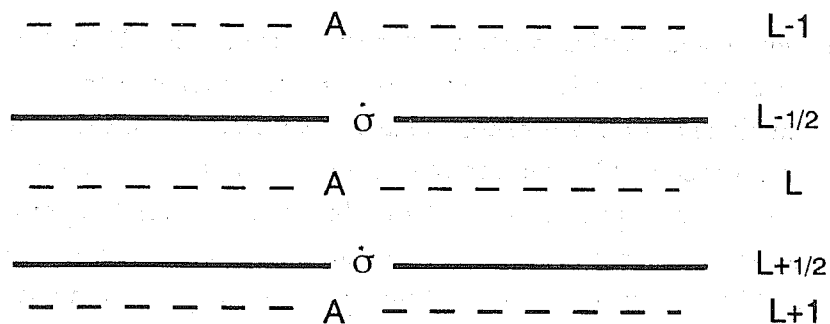


Fig. 1. Vertical indexing with variable A carried at layers ("full levels") and vertical velocity at interfaces ("half levels").

$$\hat{A}_{L+1/2} = \frac{(F'_{L+1} A_{L+1} - F_{L+1}) - (F'_L A_L - F_L)}{F'_{L+1} - F'_L}$$

A popular choice is

$$\hat{A}_{L+1/2} = \frac{1}{2} (A_L + A_{L+1}) \tag{2}$$

(Lorenz, 1960) which achieves conservation of the global integral of kinetic energy with respect to mass when the scheme is used for the horizontal velocity components. Scheme (2) along with (1) is used, for example, in the U.S. National Meteorological Center's (NMC) Medium Range Forecasting model (MRF, e.g., Sela, 1982) as well as in the NMC's Eta Model.

A legitimate argument though is that a difference scheme is defined only in terms of prognostic variables so that the introduction of interface values of  $\hat{A}$  is only a stratagem used in arriving at a scheme. In any case, insertion of e.g. (2) into (1) eliminates a reference to  $\hat{A}$  from the scheme. A Taylor-series accuracy analysis of (1) performed with values of A taken as defined at mid-points of layers then shows that for unequal values of  $\Delta\sigma$  the scheme is of a zero-order accuracy.

In judging the advantages and disadvantages of the conservation vs. accuracy features of (1) the basic question is obviously one of the meaning of the grid point values of prognostic variables. They could be looked upon as grid box averages of variables, or as values that various functions are taking at particular points in space. If they are considered grid-box averages then the Taylor-series expansion and the associated order-of-accuracy analysis are not valid. This former approach is presumably always used in physical parameterizations. Space discretization of the dynamical part of the equations on the other hand tends to be done using a mixture of the two approaches. Dynamical discretizations using one approach only are high Taylor-series accuracy / non-conserving schemes, on one hand, and constant-

volume characteristic-based schemes on the other (e.g., Carpenter et al., 1990). The latter class of schemes has no conflicts with current physical parameterizations methods, but it is not strictly applicable to multi-dimensional problems which appears particularly uncomfortable if a global model is to be designed. In any case, currently different groups are intentionally using schemes with widely varying Taylor-series accuracy and each is apparently producing encouraging results. Explanation of these results thus must be more complex than just involving the order of accuracy of the schemes used.

### 3. VERTICAL RESOLUTION

#### 3.1 Requirements in relation to the horizontal resolution

While it has been general practice to increase the vertical resolution more or less along with the increases in horizontal resolution as more powerful computers became available, a number of efforts have recently been made to assess the vertical resolution requirements for a given horizontal resolution in a more quantitative way. The ideas put forward were not only that it makes physical sense to vertically resolve systems that one is aiming to resolve in the horizontal, but even that the "excess" (Lindzen and Fox-Rabinovitz, 1989) horizontal resolution can be harmful to the forecast.

Pecnick and Keyser (1989) have presented results of simulations of upper-tropospheric frontogenesis with various horizontal and vertical resolutions. A noise problem which they encounter with "insufficient" vertical resolution is removed in their simulations with an increase in vertical resolution. A further increase in vertical resolution was of no benefit as it resulted in only slight changes in the results. The optimum vertical resolution, beyond which no significant improvement existed, was found to increase with horizontal resolution following a consistency relationship

$$\Delta z_{\text{opt}} = s\Delta y. \quad (3)$$

Here  $\Delta z_{\text{opt}}$  is the optimum vertical grid spacing in geometric height,  $s$  is the frontal slope, and  $\Delta y$  is the horizontal grid spacing.

Lindzen and Fox-Rabinovitz (1989) arrive at two consistency requirements. One is a direct application of the quasi-geostrophic vertical and horizontal scale relationship

$$\Delta z_{\text{opt}} = (f/N)\Delta y \quad (4)$$

where  $f$  is the Coriolis parameter and  $N$  the buoyancy frequency. For another, they consider gravity-inertia waves in the neighborhood of critical surfaces. The condition they arrive at involves accounting for the damping rate which they approximate by  $\nu/(\Delta z_{\text{min}})^2$ , where  $\nu$  is the vertical eddy viscosity and  $\Delta z_{\text{min}}$  the minimum vertical scale, occurring at a critical layer. They obtain

$$\Delta z_{\text{min}} \approx [(\nu/N)\Delta y]^{1/3} \quad (5)$$

An uncomfortable feature of these relationships is the dependence of the vertical resolution requirements on latitude and stability. Obviously, vertical resolution can hardly be made to change in space and time to account for these dependencies. One could, though, attempt to do this by changing the horizontal resolution (Lindzen and Fox-Rabinovitz, 1989). Dependence on the frontal slope in (3) is another disquieting point since there is no limit as to how small a frontal slope can be. Perhaps one can take some comfort in the fact that for typical grid distances used at present as well as for typical values of various parameters the requirements posed by (3) to (5) are rather similar (Persson and Warner, 1991):  $\Delta z$  in the range of about 0.5 to 2 km is obtained for grid distances of 100 km. One could derive additional comfort from the fact that the "optimum" resolution in (3) and perhaps also (4) refers to the value at which no *gain* is to be achieved in increasing the vertical resolution further, but not that any harm will come from it. Thus, a relatively high vertical resolution would appear to be a way out of some of these difficulties.

Persson and Warner present results additional to those of Pecnick and Keyser showing an appearance of noise when the horizontal resolution is increased relative to that of the control experiment, and its disappearance when the vertical resolution is also increased. Results of one of their experiments is shown in Fig. 2. Results of the control experiment are shown in the lower panel of the figure, with solid lines representing pressure vertical velocity ( $\mu\text{b s}^{-1}$ ) and dashed lines potential temperature (K). The control simulation was made with 25 model layers and a horizontal grid spacing of 30 km (S2530). Increasing only the horizontal resolution to a 10 km grid distance gave the noisy result shown in the top right panel (S2510). The noise disappeared when the vertical resolution was also increased, to 75 layers, as shown in the top left panel (S7510).

Persson and Warner suggest a simple explanation of how the violation of the requirement (3) might lead to the formation of spurious gravity waves. The schematic they use is reproduced in Fig. 3. It shows a narrow sloping front (shaded region) with relative temperature values at model grid points, T2 and T1, where  $T2 > T1$ . The pressure levels are indicated at the left of the bounded region ( $P3 > P2 > P1$ ) and the relative magnitudes of the geopotential height at the top of it ( $H4 > H3 > H2 > H1$ ). With the geopotential height change occurring in every third grid column, generation of spurious gravity waves is to be expected.

Lindzen and Fox-Rabinovitz warn that "virtually all large scale models ... have inadequate vertical resolution". In contrast, the "fine vertical / fine horizontal" resolution of Persson and Warner (S7510) is not really more demanding than what is typically used in operational and soon-to-be operational models. Thus, the operational regional forecasting model of the U.S. National Meteorological Center (Hoke et al, 1989) with its horizontal grid distance of about 80 km has 16 layers in the vertical, more than 1/8 of 75 which would correspond to Persson and Warner's S7510 experiment. The same horizontal and vertical resolution is used at NMC for the current semi-operational version of the Eta Model. However, some of the

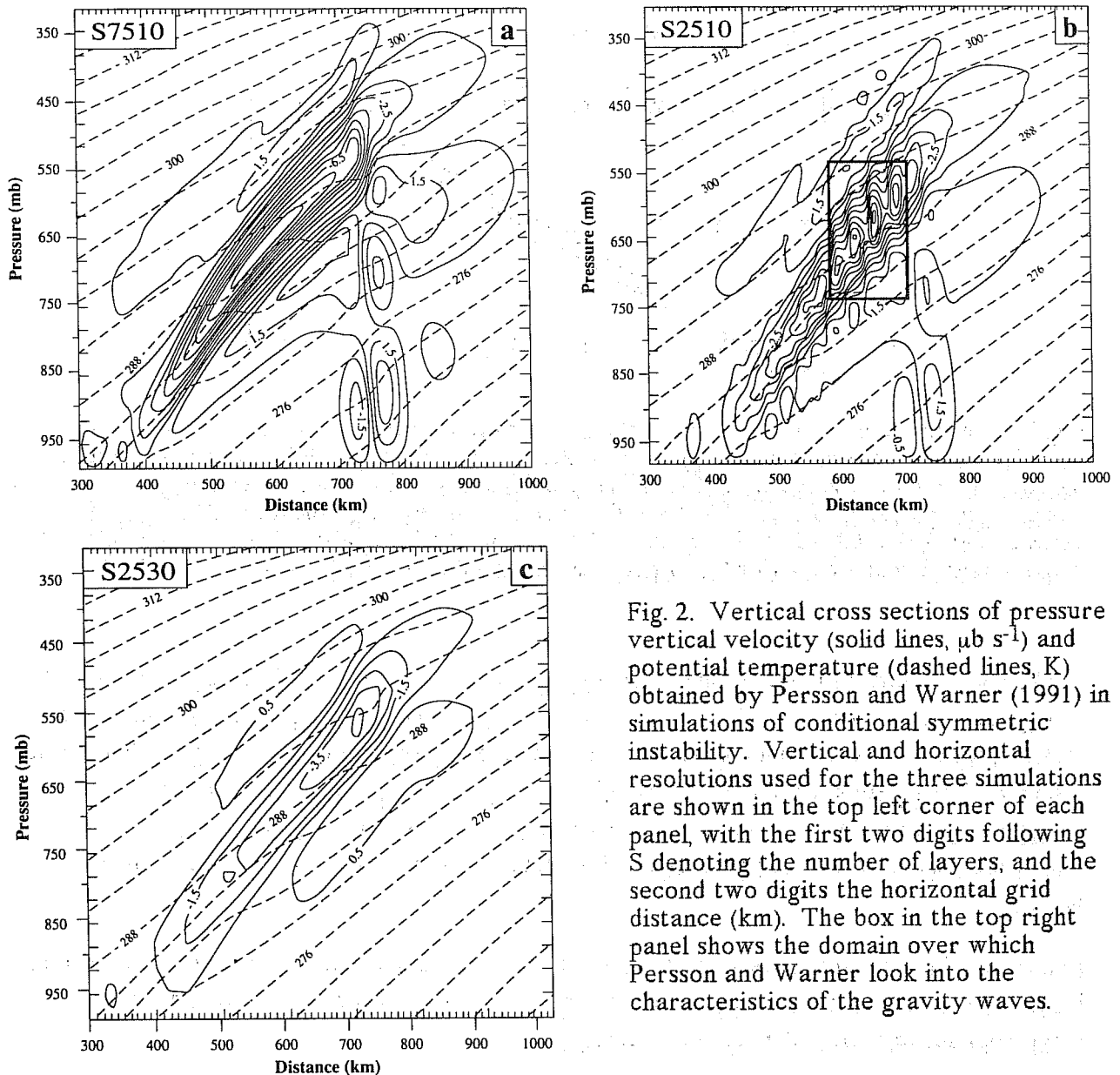


Fig. 2. Vertical cross sections of pressure vertical velocity (solid lines,  $\mu\text{b s}^{-1}$ ) and potential temperature (dashed lines, K) obtained by Persson and Warner (1991) in simulations of conditional symmetric instability. Vertical and horizontal resolutions used for the three simulations are shown in the top left corner of each panel, with the first two digits following S denoting the number of layers, and the second two digits the horizontal grid distance (km). The box in the top right panel shows the domain over which Persson and Warner look into the characteristics of the gravity waves.

layers are spent to achieve an increased resolution near the ground surface. Also the distribution of layer thicknesses is not uniform in  $z$  above the atmospheric boundary layer. These are the subjects of the following sub-section of this lecture.

### 3.2 Distribution of layers / levels

Optimizing the vertical distribution of layers has been a constant concern of modelers and has been approached from a number of points of view. Analyses too numerous to specifically mention here show it best to have layers of equal thickness in terms of the model coordinate when considering accuracy of vertical discretizations. Since for meteorological reasons variable layer thicknesses are typically used, minimization of the vertical change in layer

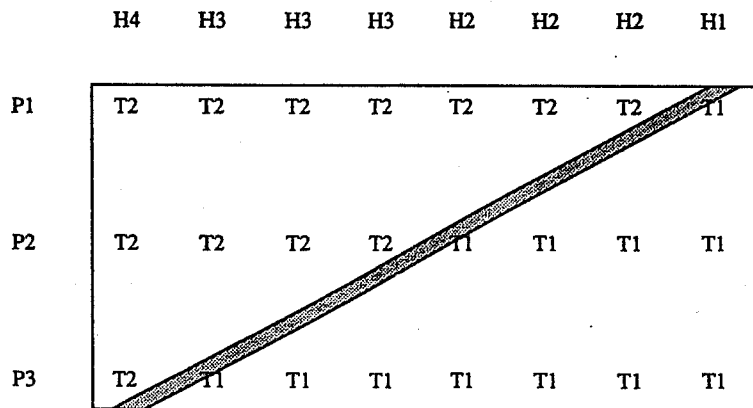


Fig. 3. Schematic of the mechanism of the generation of spurious gravity waves due to insufficient vertical resolution suggested by Persson and Warner (1991). Cross section of a narrow sloping front is indicated by the shaded region, and the relative temperature values at various grid points by T2 and T1 ( $T_2 > T_1$ ). Pressure levels are indicated at the left of the cross section ( $P_3 > P_2 > P_1$ ). Integration of the hydrostatic equation will lead to geopotential heights changing at every third grid point, as indicated on top ( $H_4 > H_3 > H_2 > H_1$ ).

thicknesses is practiced. For example, in conjunction with an increase in resolution, a rapid change in layer thicknesses which existed in the NMC's Medium Range Forecast model at mid-troposphere (e.g. Kanamitsu, 1989) is currently being replaced by a smoother distribution (Mark Iredell, personal communication). When using conserving schemes, avoiding rapid changes in layer thicknesses in terms of mass may be particularly desirable because compensations in various physical quantities occur in interactions between neighboring layers.

Linear stability requirements with thin layers is yet another matter related to the choice of layer thicknesses. It has recently been shown to be a factor which can limit the efficiency of a non-split scheme (Hortal, these proceedings).

Arakawa and Lamb (1977) have found it possible to determine layer thicknesses so as to avoid false internal reflection of wave energy in case of an isothermal atmosphere. They considered a particular scheme in which a false reflection was prevented when layer thicknesses were chosen equal in  $\log p$ .

By far the most frequent considerations when choosing layer thicknesses are those of presumed model "physics" requirements. Boundary layer parameterizations are generally considered particularly demanding. Typically, a fairly thin surface layer (10-20 m) and a total of at least 4-5 layers in the boundary layer are considered desirable. Processes thereby aimed to be simulated are the growth and decay of the daytime boundary layer and maintenance of a nearly well-mixed layer in the oceanic boundary layer (Hua-Lu Pan,



personal communication). The jet-stream/tropopause level and the top of the model atmosphere are regions where increased vertical resolution is also frequently considered desirable.

A need to better understand these issues is underscored by the fact that the eta vertical coordinate now used by a number of groups by design cannot accommodate multiple thin layers next to the ground surface above elevated terrain. Conceivably, the need for a high resolution in the boundary layer can be eliminated or ameliorated by an increased sophistication of the boundary layer parameterizations. In this connection, existence of a nested boundary layer approach should also be noted (Thompson and Burk, 1991). In this approach a high-resolution vertically nested model is used in which changes due to its physics are layer averaged at the end of each time step and supplied to a coarse grid resolution model.

With such a large number of diverse considerations at play, some of which are hardly subject to mathematical arguments, the choice of the distribution of layer thicknesses remains a highly empirical subject. Understanding of various concerns should provide useful guidance as to which features of a model's performance should receive special attention.

#### 4. COORDINATE SYSTEMS

##### 4.1 The isentropic coordinate

The simplicity and the aesthetic appeal of the normalized pressure, or "sigma" vertical coordinate of Phillips (1957) has been such as to ensure it a most widespread use. Above the ground surface the sigma coordinate however does little to take advantage of the physical nature of atmospheric motions. The most radical effort in attempting to benefit from the known characteristics of large-scale atmospheric motions is undoubtedly the choice of the isentropic coordinate. It makes adiabatic motion a two-dimensional problem and it automatically allows for an increased resolution of atmospheric frontal zones both of which offer substantial potential rewards in the accuracy of simulations. Thus in spite of inherent technical difficulties the isentropic coordinate continues to attract strong interest among atmospheric modelers. This interest appears to be on the increase in recent years.

Following the first successful integration of the primitive equations by Eliassen and Raustein (1968) numerous developments have taken place which have established isentropic modeling as competitive to other state-of-the-art choices of vertical coordinate. To reduce problems with the lower boundary frequently a hybrid coordinate system is used, with a sigma coordinate subdomain near the ground surface (e.g., Black, 1987). While historically a number of approaches have been used, the technical problem of the intersection of isentropic coordinate surfaces with the ground surface or with the uppermost sigma interface is at present commonly handled by the "massless layer" approach (e.g., Hsu and Arakawa, 1990; pioneered by Bleck, 1984). In this approach isentropic layers are extended along the ground

surface or along the uppermost sigma interface with their mass going to zero at places where they would be discontinued were they to be required to have a mass greater than zero.

Regarding the calculation of the pressure gradient force, the isentropic coordinate avoids the problem the terrain-following coordinate has with the simulation of the resting atmosphere above sloping terrain; it does not however avoid the need to observe the condition of hydrostatic consistency (Mesinger and Janjić, 1985). For further discussion of the issues of the pressure gradient force with the isentropic coordinate the reader is referred to Mattocks and Bleck (1986).

As an illustration of both the strong and the weak points of isentropic modeling I shall show two recent results of Konor et al. (1991). They have performed simulations of frontogenesis using a sigma and an isentropic model making an effort to have the two models as similar as practically possible except for the difference in the vertical coordinate. Initial conditions in each case consisted of a single jet centered at mid-latitudes and the wind field in a gradient or a geostrophic balance as appropriate. Simulations were started with small perturbations superimposed upon the zonal flow. For the  $\sigma$ -model simulation the origin of time was chosen at the end of a period during which interaction with the zonal flow was prevented in order to allow for the organization of the perturbation into the most unstable structure of the linear system.

The geopotential height and the potential temperature ( $\theta$ ) fields at 500 mb and 950 mb levels that Konor et al. obtained at day 3.5 and at day 5 of their  $\sigma$ -simulation are shown as the top (500 mb) and as the middle (950 mb) panels in Fig. 4. Lines denoted by A and B in these panels show locations at which vertical cross sections of  $\theta$  and potential vorticity (PV) were taken and are shown as the bottom panels of the figure. At day 3.5 in the middle left hand panel a weak warm front can be seen at 950 mb east of the low pressure center. At day 5 to the right of that panel the warm and cold fronts are well developed forming a typical "T-bone" structure. Associated with this is a frontal zone that can be observed in the upper troposphere in the day 5 cross section with a high PV tongue extending from the stratosphere into the middle troposphere.

These and other various features of Fig. 4 can be compared against those of Fig. 5 in which results of the  $\theta$ -simulation are shown. Intense temperature gradients are seen at the upstream sides of the 500 mb troughs at both days 6 and 9. At 950 mb surface frontal features do not appear realistic however. At day 6 at the vertical cross section across the frontal zone (bottom left panel) a narrow high PV tongue extends from the stratosphere into the middle troposphere. It is penetrating still deeper at day 9. Associated with it is a very sharp frontal zone in the upper troposphere. On the basis of these features and their results of the evaluation of the terms of the frontogenetical equation Konor et al. conclude that the  $\theta$ -model is much more successful than  $\sigma$  in capturing the details of the frontal-scale dynamics in the

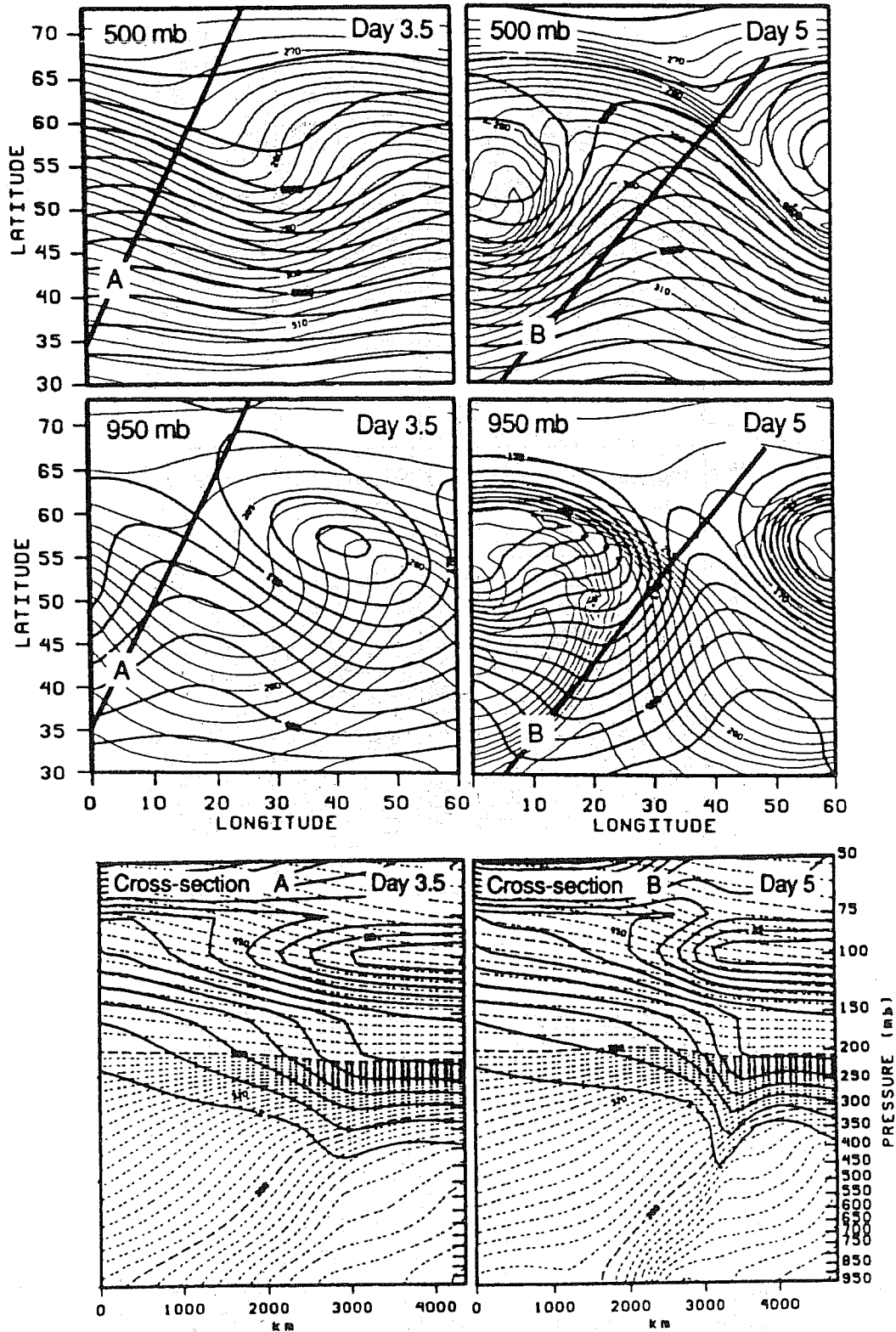


Fig. 4. Geopotential height (m, thick lines) and the potential temperature (K, thin lines) Konor et al. (1991) obtained at day 3.5 and at day 5 of their  $\sigma$ -simulation: 500 mb top panels, 950 mb middle panels. Lines denoted by A and B show locations at which vertical cross sections of  $\theta$  and potential vorticity (PV) were taken and are shown as the bottom panels ( $\theta$ , dashed lines; PV, solid lines).

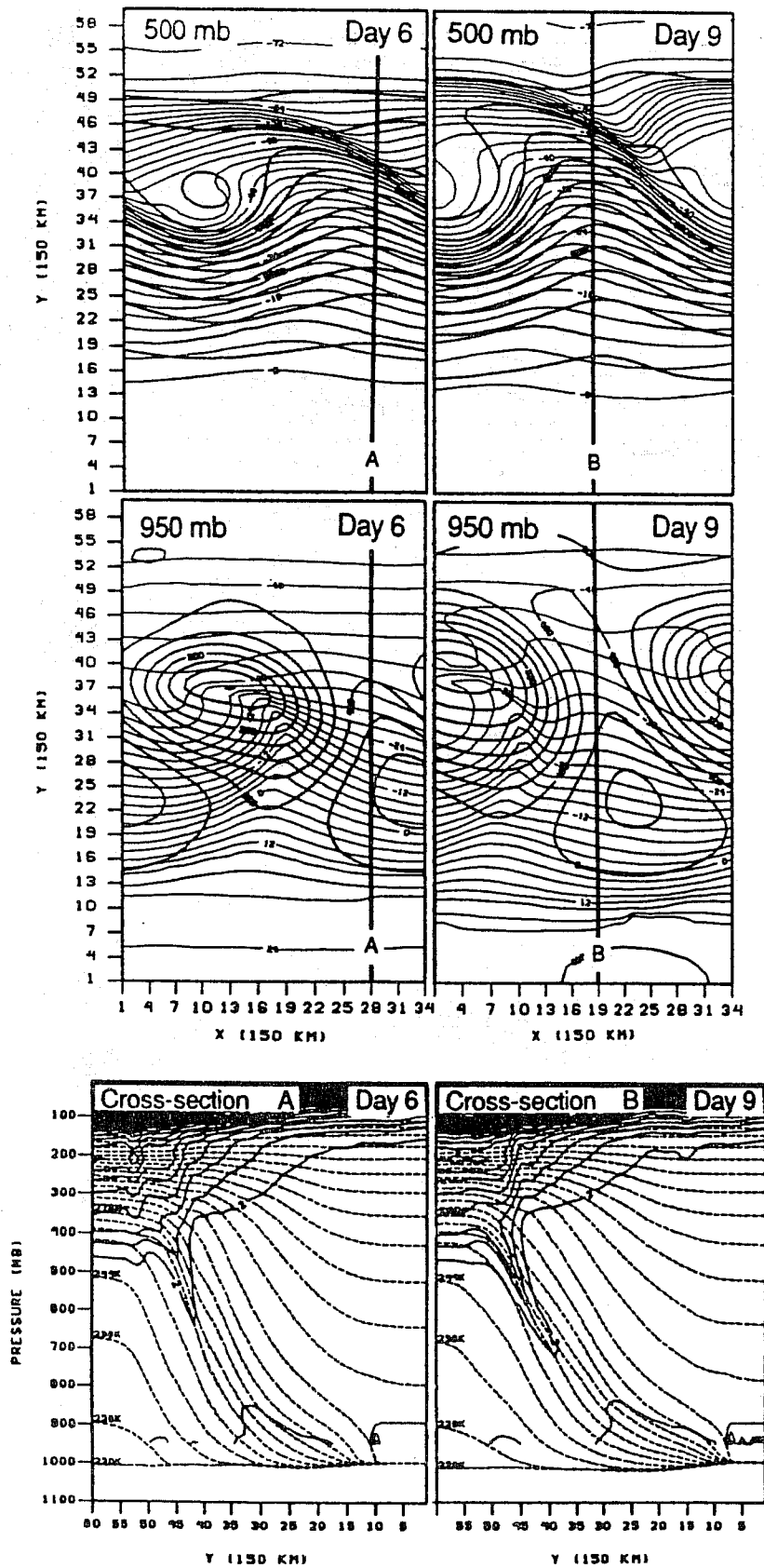


Fig. 5. As in Fig. 4 except for days 6 and 9 of the  $\theta$ -model simulation (Konor et al 1991).

upper troposphere. They conclude that a combination of the  $\sigma$ - and the  $\theta$ -model should be useful in the attempt to adequately simulate the frontogenetical processes both at the surface and in the upper and middle troposphere.

As already pointed out, such an approach is indeed frequently taken. For more recent references on this technique the reader is referred to Pierce et al (1991) and Benjamin et al (1991). Isentropic-only modeling has not been abandoned though; see, e.g., Tafferter and Egger (1990).

#### 4.2 The step-mountain (eta) coordinate

Various problems associated with the use of the terrain-following ("sigma") coordinate have been discussed at some length in a previous ECMWF seminar paper (Mesinger and Janjić, 1987). The problem of possible errors in calculation of the pressure gradient force was the one of greatest concern. In spite of an extraordinary number of papers during more than two decades published on the topic, this subject has continued to attract the interest of atmospheric and ocean modelers (e.g., Carroll et al, 1987; Achtemeier, 1991; Haney, 1991; see also Mesinger et al, 1988b).

The pressure gradient and other problems of the sigma coordinate are caused by the slope of coordinate surfaces. The hybrid coordinate of Simmons and Burridge (1981) progressively reduces the slope of coordinate surfaces as the elevation increases above ground surface. A still more radical effort is the use of the step-mountain ("eta") coordinate (Mesinger, 1984) forcing coordinate surfaces to be approximately horizontal at all elevations. This is achieved at no loss in technical simplicity compared to the sigma coordinate. A possible disadvantage already pointed out is that by design the coordinate cannot accommodate multiple thin layers next to the ground surface above elevated terrain.

One attractive feature of the eta coordinate is that a simple redefinition of its ground surface values to unity at all grid points makes it a sigma coordinate. This allows the same model code to be run both as the eta and as a sigma model thus enabling experimentation aimed at determining the benefit, if any, from the use of the eta vs. sigma coordinate. Early experiments of this kind by Mesinger et al (1988b) using a dry "minimum physics" model revealed a substantial amount of noise associated with the use of the sigma coordinate. The noise was presumed to reflect the numerical errors resulting from the use of the coordinate. Following development at NMC of a comprehensive physics package for the Eta Model (Janjić, 1990) several eta/sigma experiments with the full-physics model indicated that some degradation of the short-range forecast accuracy might also be resulting from the use of the sigma coordinate (Mesinger et al, 1988a). For a number of reasons results of these experiments were not very conclusive.

As there was a need for additional experiments of this kind, Tom Black of NMC and I have

recently performed three forecasts both in the eta and the sigma mode; results will be presented here. We have chosen the cases for these comparisons in which the forecasts might be particularly sensitive to the choice of the vertical coordinate. We chose from 5 or 6 cases for which the initial and the boundary conditions were readily available those in which processes related to mountains seemed more important than in the remaining cases.

I will refer to the cases chosen as those of February 89, April 91, and May 91. The February 89 case is one involving a very intense cold air outbreak east of the Rockies which I have already discussed at the ECMWF seminar of two years ago (Mesinger and Janjić, 1990, Subsection 9.1). The April 91 case was chosen to study the propagation of a low that crossed a major part of the Rockies during the 48-h forecast. The files for the May 91 case we had available because of our effort to produce a cover illustration for the preprint volume of the American Meteorological Society's 9th NWP Conference; for that purpose we had been looking for a case associated with substantial precipitation in the area of Denver, Colorado, the site of the conference. The case also satisfied our requirement of involving an event related to mountains since Denver is at a high elevation and in the proximity of still higher mountains.

The most recent version of the NMC Eta Model was used for our eta/sigma experiments; for model changes subsequent to those covered by the Janjić (1990) paper the reader is referred to the paper by Mesinger, Black and Janjić, from these proceedings. The model version used was our "standard" resolution version of about 80 km grid distance and 16 layers in the vertical. This grid distance, vertical resolution and the version's domain size were chosen in order to have the model's computing effort comparable to that of the U.S. operational regional model (Nested Grid Model, NGM, Hoke et al., 1989). The mountains in this Eta Model version are shown in Fig. 6. In this figure dots denote the water points; note that we have no mountains along the two outermost lines of grid points. Note, furthermore, that terrain elevation is defined to be the same for groups of four neighboring height grid points. This latter feature is a choice we have made partly for reasons of convenience as a simple way of avoiding isolated height (surface pressure) points surrounded on all four sides by mountain walls.

The February 89 Case. The reason we originally became interested in this severe cold air outbreak east of Rockies was a spectacular failure of the U.S. operational regional model (NGM) in forecasting the southward movement of the cold air. In two consecutive 12-h cycles, forecasts from the operational model developed a deep anomalous low centered approximately at the Nebraska-Wyoming-Colorado border which blocked the cold air and even moved it back northward in contrast to the observed southward movement of cold air with no low in the region (e.g., Mesinger and Janjić, 1990). As the Eta Model did not develop a false low it was a matter of obvious interest to find out to what extent this was associated with the use of the step-mountain coordinate.

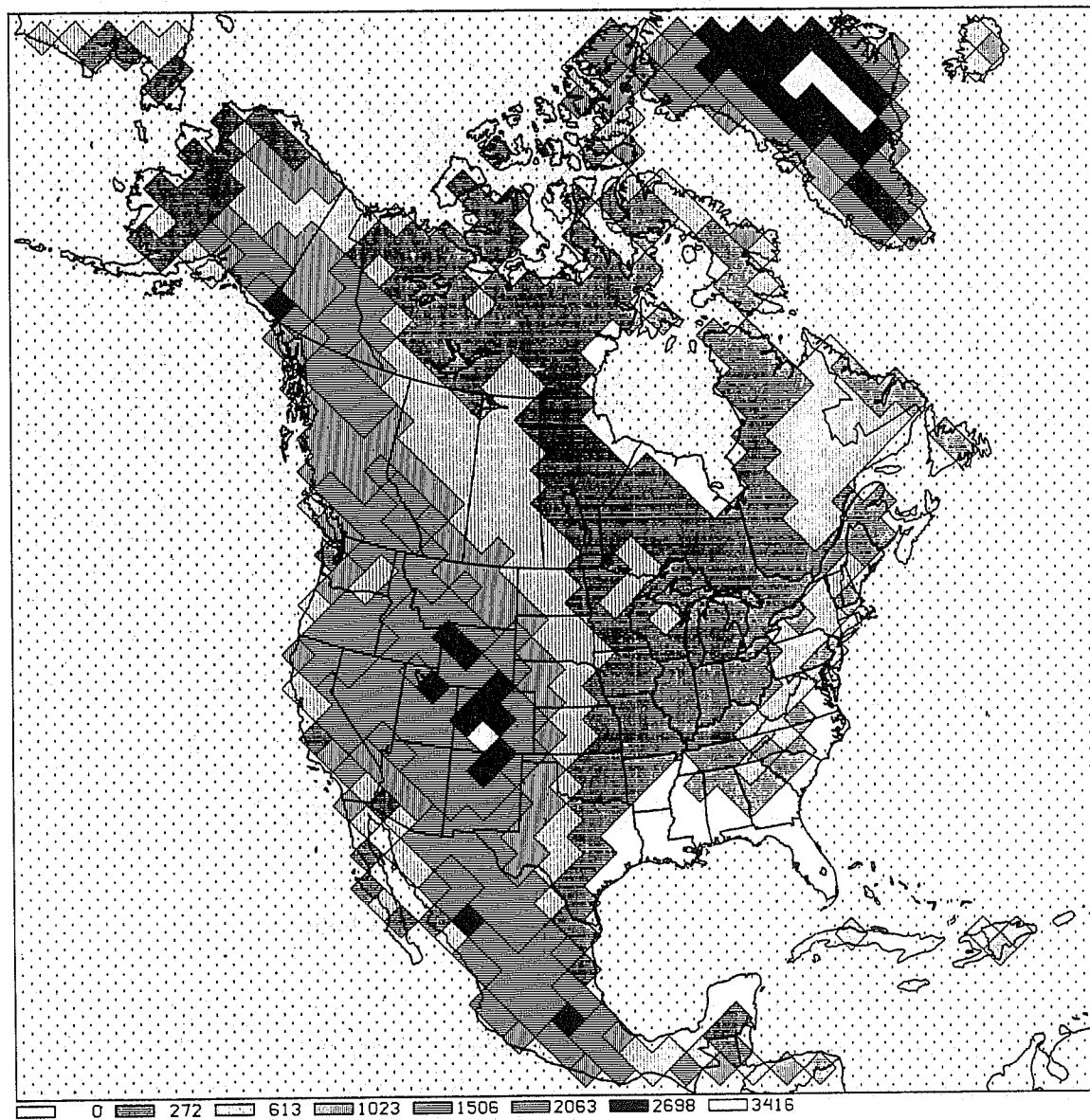


Fig. 6. Topography (m, as shown in the legend at the bottom of the plot) and location of the water grid points (dots) of the 80-km 16-layer version of the NMC Eta Model.

A section of the NMC surface analysis for 0000 UTC 3 February 1989 with the cold air already well to the southeast of the Rockies is shown in Fig. 7. Extremely cold temperatures were reported at various stations, such as  $-33^{\circ}\text{F}$  in northern Wyoming; and temperatures well below freezing occurred in states as far south as Texas (e.g.,  $11^{\circ}\text{F}$  at a Texas panhandle station).

The two Eta Model 48-h forecasts of the sea level pressure and 1000-500 mb thickness verifying at the same time are shown in Fig. 8. The sigma mode forecast is shown in the upper panel and the eta mode forecast in the lower panel of the figure. The Eta Model's

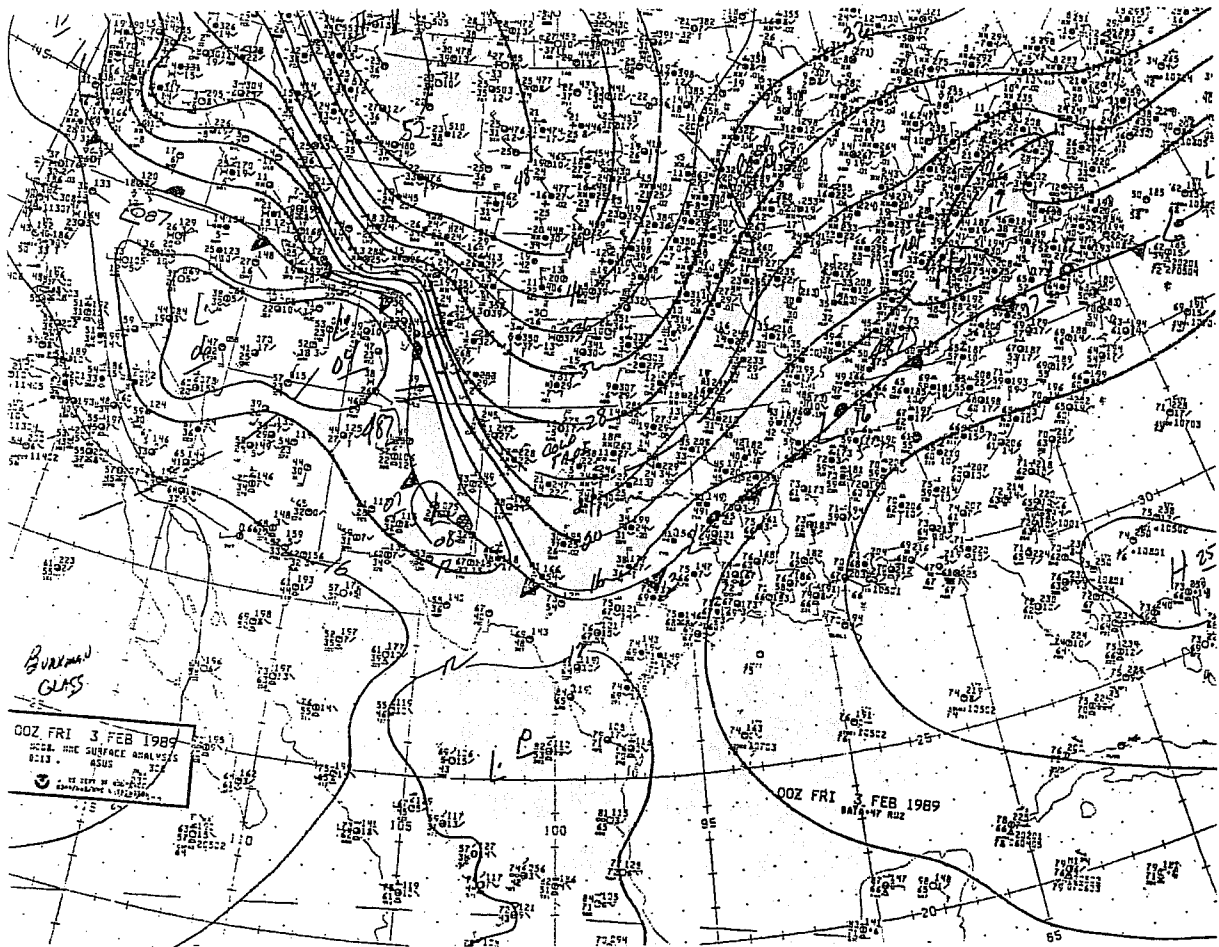


Fig. 7. A section of the NMC surface analysis for 0000 UTC 3 February 1989.

reduction to sea level using horizontal relaxation-deduced interpolation of virtual temperature under terrain (Mesinger, 1990) is not available for the sigma mode; both maps therefore use the "standard" reduction to sea level. It is based on the lowest layer temperature and the standard atmosphere lapse rate of .65 K/100 m.

While the overall appearance of the two sea level pressure plots is rather similar, a closer inspection does reveal some systematic differences. Taking sea level pressure values at Midwestern states as indicative of the advance of the cold air one can note that in the eta mode forecast the cold air has progressed further to the south and southeast than in the sigma mode forecast. For example, the two isobars running across the two eastern corners of South Dakota are each 4 mb higher in the eta mode forecast than in sigma. Pressures are still higher in the analysis; thus, the eta mode forecast was more successful in moving the cold air southward and southeastward. This might appear surprising since the extremely cold and thus shallow layer would be more poorly resolved in the eta mode where there was a smaller number of layers above mountains. For example, over central North and South Dakota (Fig.



Mesinger, Fedor: Vertical Discretization and Coordinate Systems

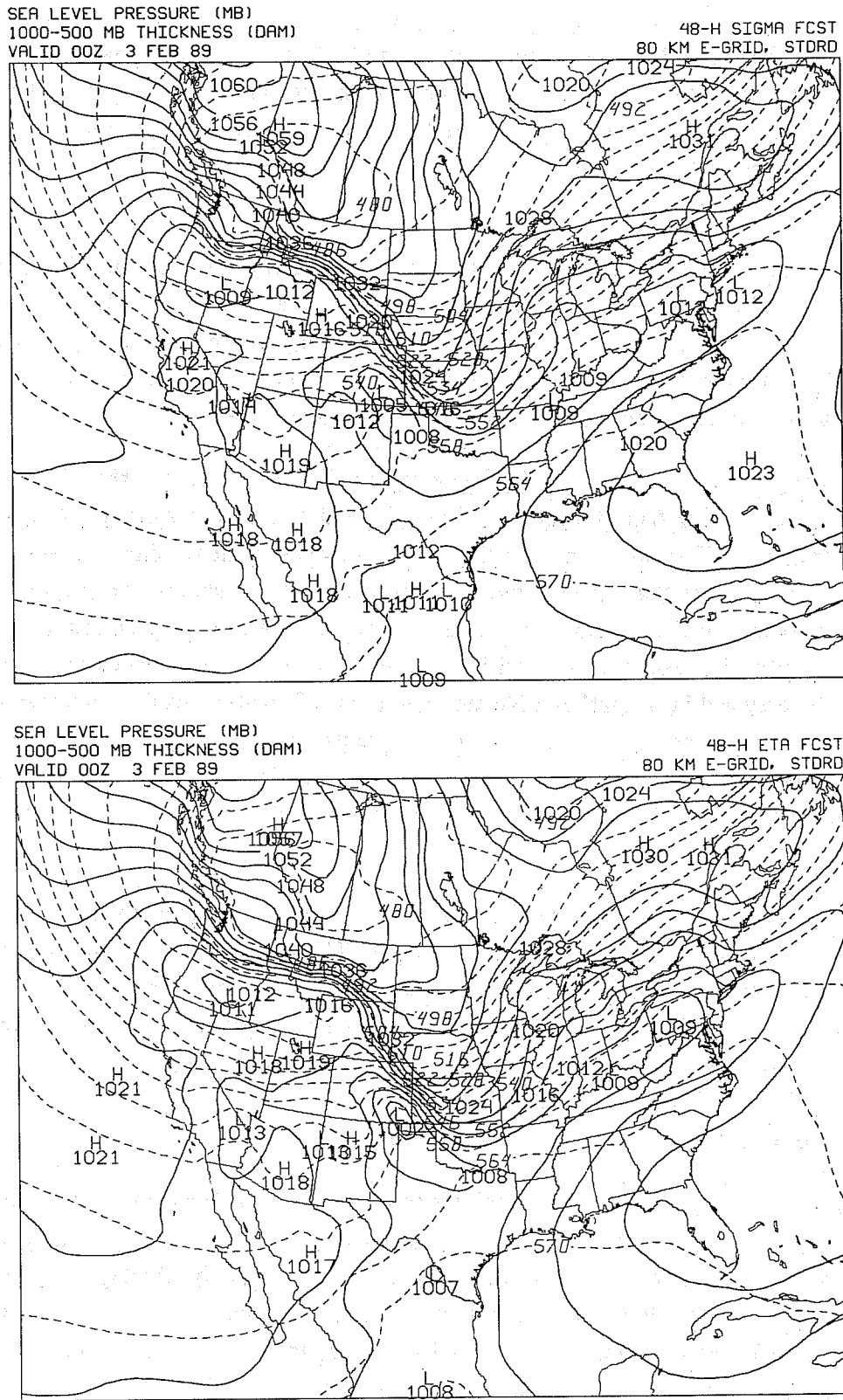


Fig 8. 48-h forecasts of sea level pressure (mb, solid lines) and 1000-500 mb thickness (dam, dashed lines), obtained running the Eta Model in the sigma mode (upper panel) and in the eta mode (lower panel), verifying at 0000 UTC 3 February 1989.

6) the eta mode had only 14 layers compared to the 16 layers of the sigma mode. We see no alternative to the conclusion that the advantages of the eta mode scheme over the sigma system outweighed the errors it incurred due to its lower vertical resolution, even though it would seem reasonable to expect errors due to insufficient vertical resolution to be particularly large in this case.

Values of pressure reduced to sea level only partly reflect the mass distribution in the two simulations since these values are also affected by the rather arbitrary rules of the reduction. For a look at the actual difference in the mass distribution free of the reduction effect, differences in surface pressure between the eta and the sigma mode integrations are shown in Fig. 9. The upper panel of the figure shows the 36 h and the lower panel the 48 h difference.

Large scale patterns can be noted in the figure with differences greater than 2 mb at 36 h covering a belt extending from Oregon to Nebraska and then northwards to North Dakota and southern Manitoba. Differences greater than 4 mb are present in Washington and most of Nebraska. Values of less than -2 mb cover northern Alberta, Saskatchewan and Manitoba and extend further into the Northwest Territories and adjacent parts of Hudson Bay. A similar overall situation exists at 48 h with the area covered by differences greater than 2 mb shifting southwestward into northern Nevada and most of Utah as well as eastward covering all of Minnesota, Iowa and Wisconsin. As already pointed out, the southward movement of the cold air was still more intense than the one reproduced in the eta simulation. The two difference plots thus reveal a large scale error reduction achieved by the eta as compared to the sigma simulation.

A point of particular interest may be the location of the area of maximum differences at 36 h, reaching more than 6 mb in southwestern Nebraska. This is the same location as that of the false large-scale low dominating the 36-h forecast of the U.S. operational regional model, shown in Fig. 10. We see this as an indication that the sigma system error in our 36-h difference map may be the same type of error as the one which triggered the false development of Fig. 10, only that in the Eta Model it was not able to have such a destructive effect as it had in the NGM because of other differences in the two models.

The April 91 Case. The NMC surface analysis to be used as verification in this case is shown in Fig. 11. The low that was suspected of being influenced by the choice of the eta vs. sigma coordinate is centered in central Texas and is analyzed at 1001 mb. During the preceding 48 h of our forecast period this low had slowly moved from southern Utah across Colorado and New Mexico into Texas. The major low over New York and the New England states analyzed at 992 mb is the low which originally prompted our interest in this case but is not one of primary concern in the present experiment.

The 48-h sigma and the eta mode forecasts verifying at the same time are shown in Fig. 12 as

Mesinger, Fedor: Vertical Discretization and Coordinate Systems

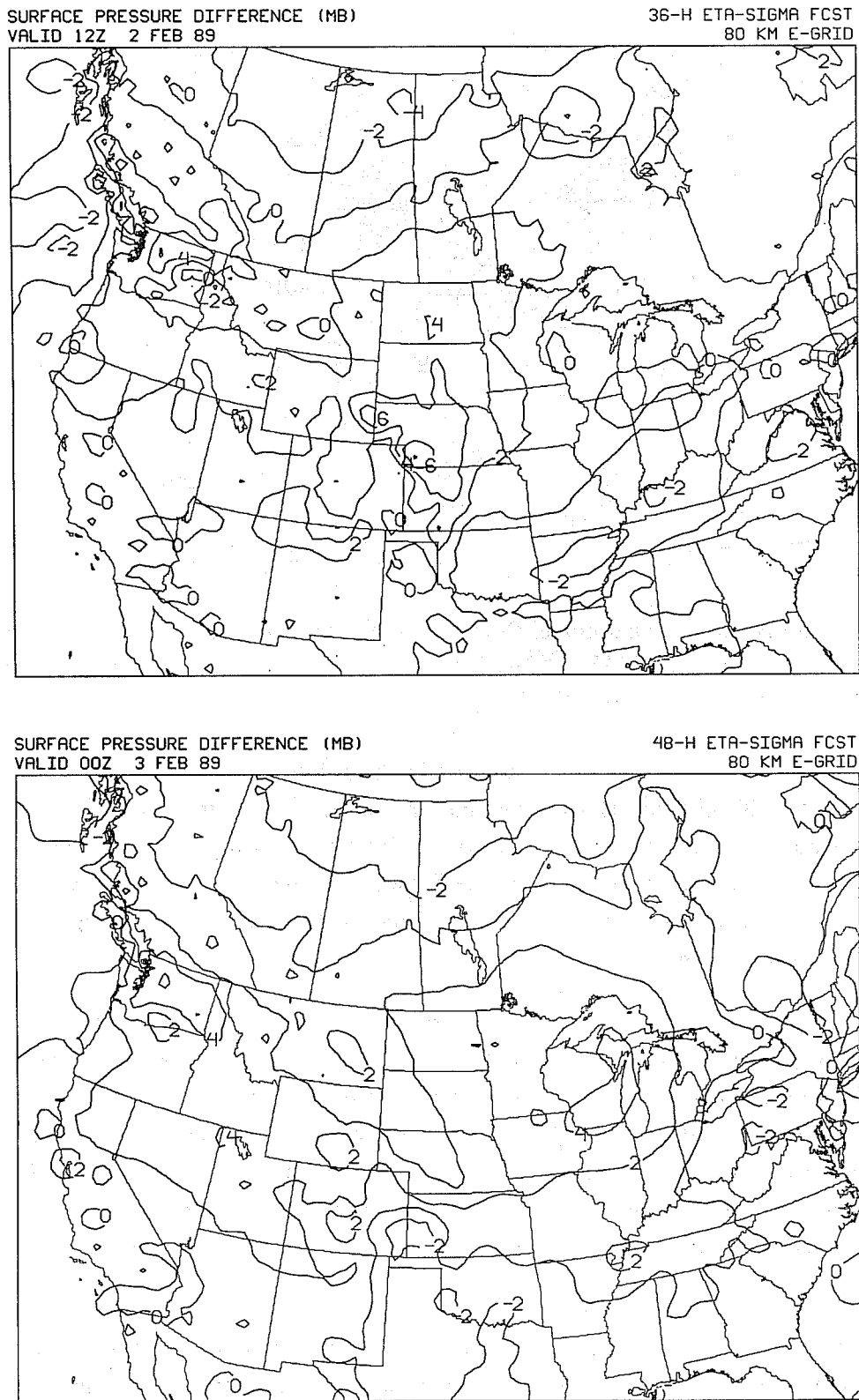


Fig. 9. Differences in surface pressure between the eta and the sigma mode integrations of the Eta Model at 36 h (upper panel) and at 48 h (lower panel), verifying at 1200 UTC 2 February and 0000 UTC 3 February 1989, respectively.

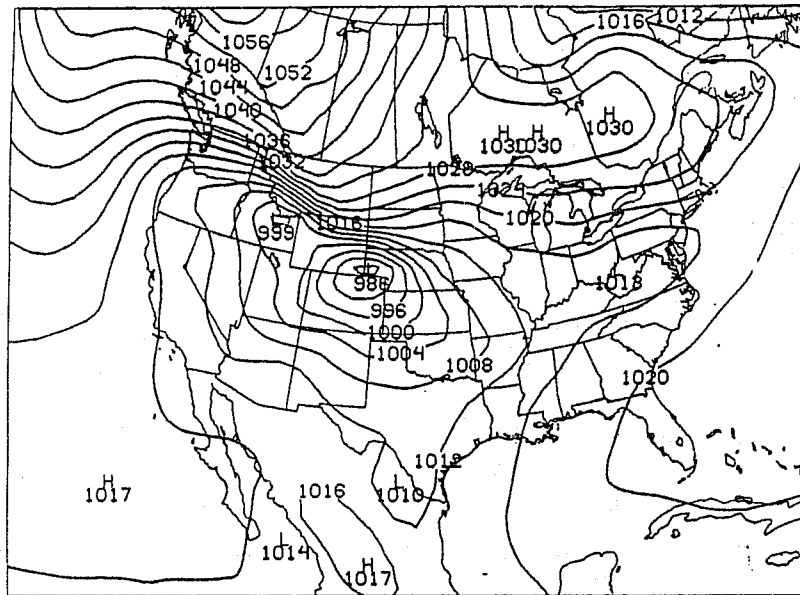


Fig. 10. U.S. operational regional model (NGM) 36-h forecast of sea level pressure (mb) verifying at 1200 UTC 2 February 1989.

the upper and the lower panel, respectively. As in the previous case, forecasts of the sea level pressure (mb) and 1000-500 mb thickness (dam) are shown. The sigma mode forecast is somewhat inaccurate regarding the location of the Texas low, placing its center at the Oklahoma-Texas border rather than in central Texas. The error is removed by the use of the eta coordinate. The central pressure of the eta forecast low (997 mb) is also more accurate than that of the sigma forecast (995 mb).

I shall again compare the two forecasts with a forecast of the NMC operational regional model (NGM) which is another sigma model run at about the same resolution. The 48-h NGM forecast verifying at the same time as the forecasts in Fig. 12 and thus using the same initial condition is shown in Fig. 13, upper panel. The location and depth errors of the Eta Model / sigma mode forecast of the Texas low are also present in the NGM forecast, and are even somewhat greater; the low is forecast still further to the north and is slightly deeper (994 mb) than the sigma low of Fig. 12.

For a check on the sensitivity of the error of the two sigma forecasts to perturbation of the initial conditions, the 36-h NGM forecast verifying at the same time is shown in the lower panel of Fig. 13. In spite of the 12-h later initial conditions the error in forecasting the Texas low remained essentially the same. Incidentally, the forecast of the position and depth of the low centered over New York did improve substantially so that it is now virtually error-free and superior to the two Eta Model 48-h forecasts.

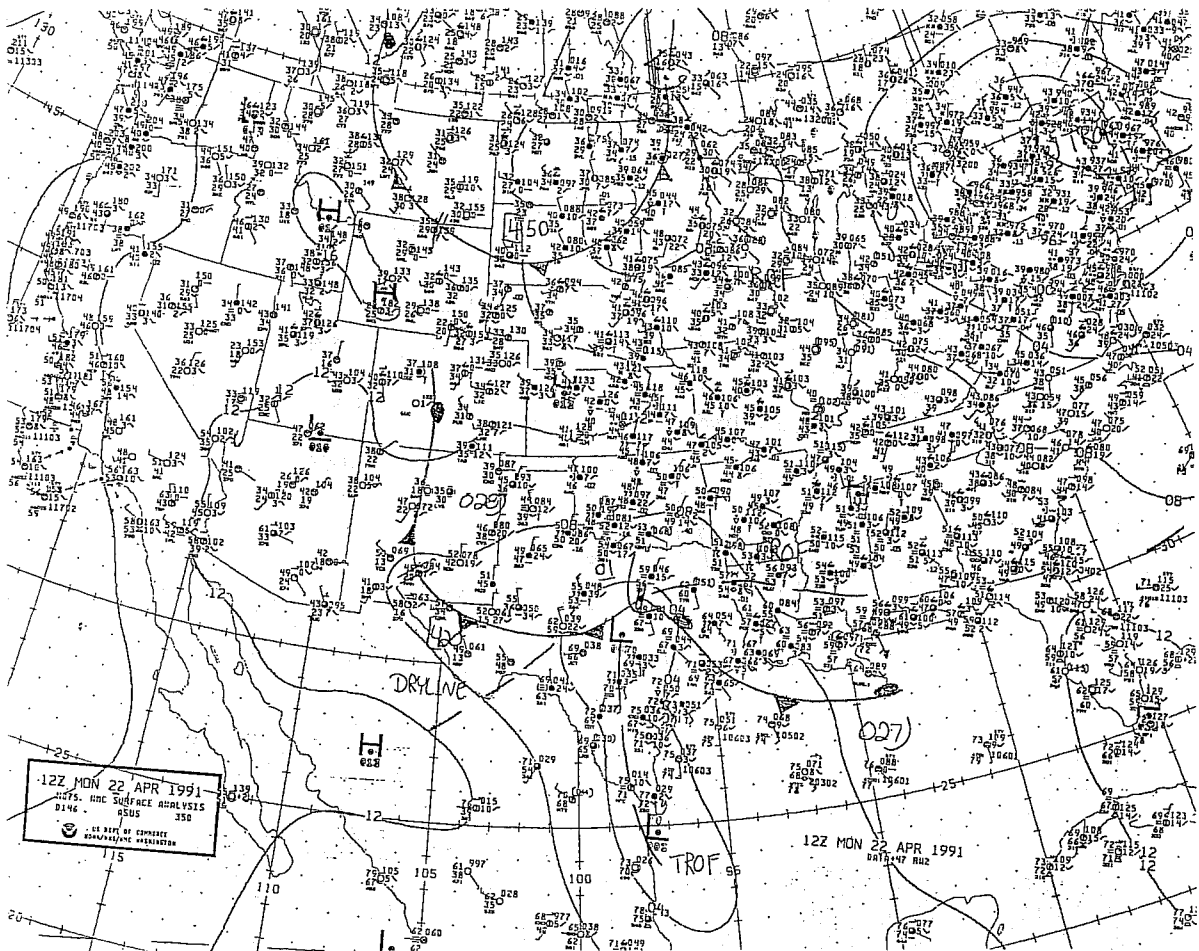


Fig. 11. A section of the NMC surface analysis for 1200 UTC 22 April 1991.

The error in forecasting the position and depth of the low over southern-central states is almost identical in the three forecasts in sigma coordinates made using two different models and two 12-h apart initial conditions. I find that this strongly supports the notion that the error derived from the use of the sigma coordinate as opposed to its resulting from the chaotic component which is unavoidably present in any two different integrations.

The May 91 Case. The NMC 48-h verification analysis of this case is shown in Fig. 14. A complex trough system runs from the southwestern states northward and then eastward across the Great Lakes area. The minimum pressure along this trough analyzed at 1003 mb over Oklahoma does not represent a center of a well-defined low, however, and is thus not so useful for verification purposes.

The 48-h sigma and eta mode Eta Model forecasts shown in the upper and lower panels in Fig. 15, respectively, do not exhibit a conspicuous difference in this instance. One difference which might deserve attention is in the position of the axis of the ridge over Wyoming,

Mesinger, Fedor: Vertical Discretization and Coordinate Systems

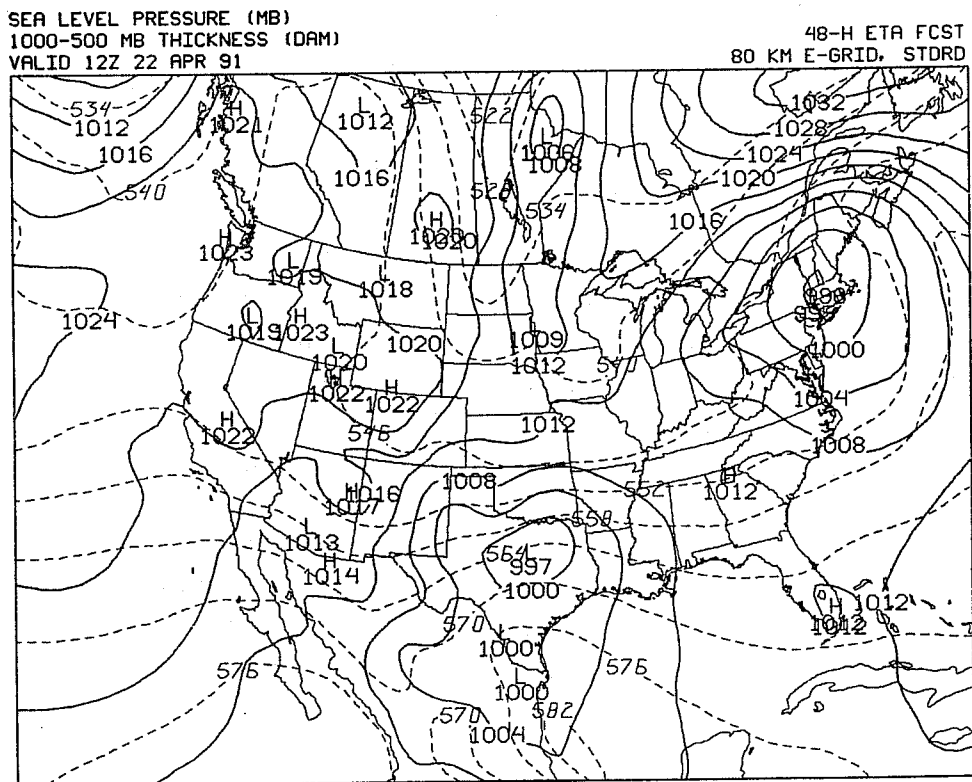
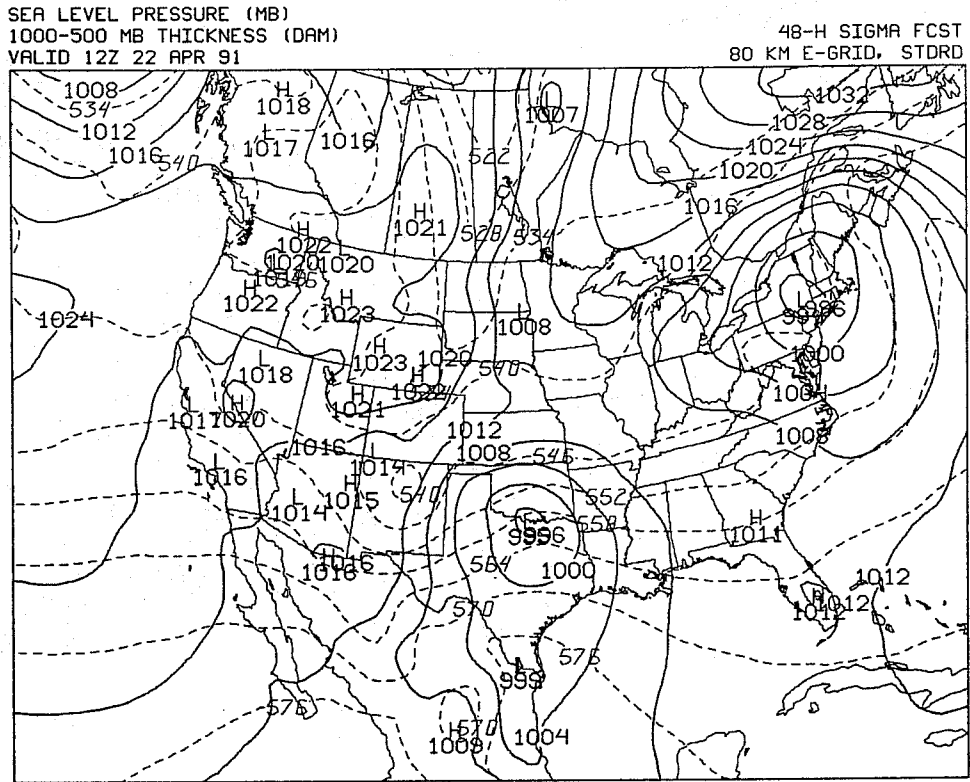
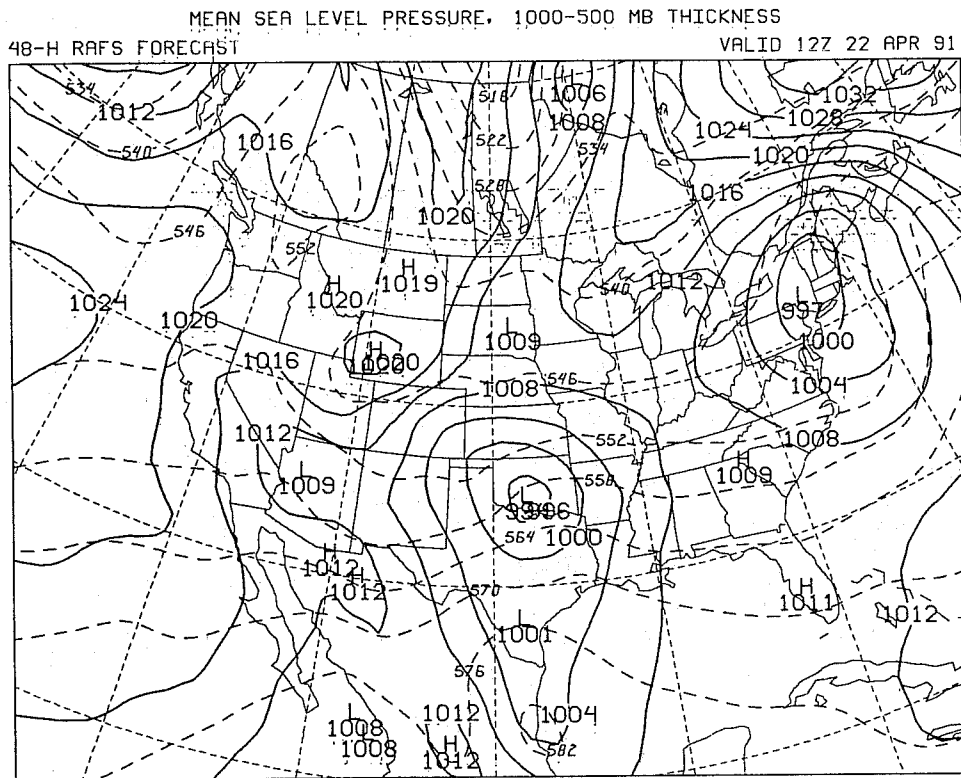
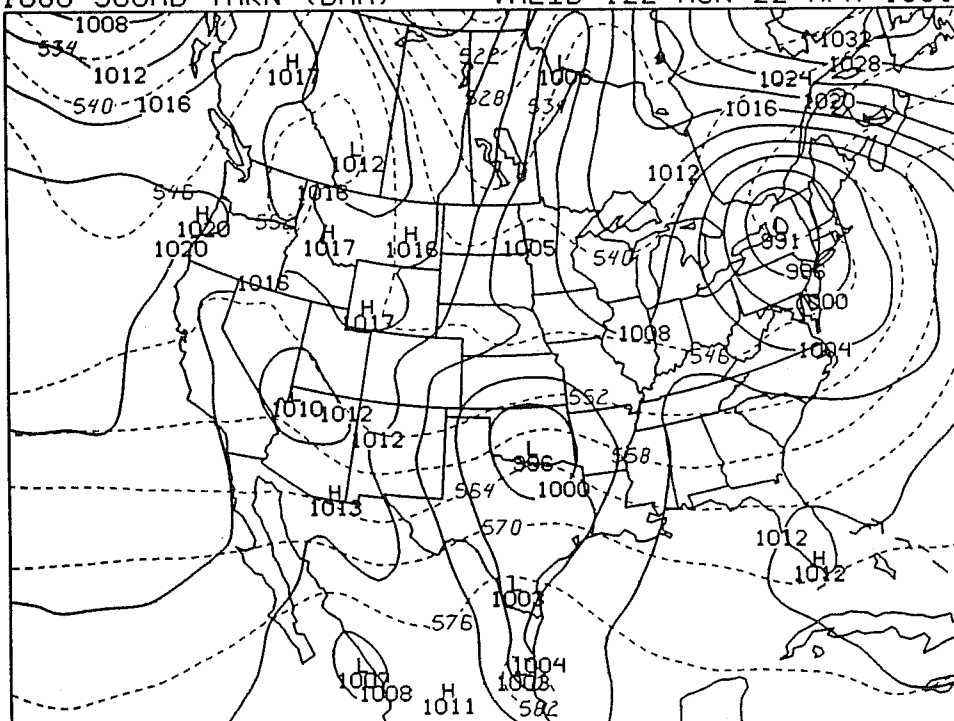


Fig 12. As in Fig. 8 except for verifying at 1200 UTC 22 April 1991.

Mesinger, Fedor: Vertical Discretization and Coordinate Systems



MSL PRESSURE (MB) ----- VALID 12Z MON 22 APR 1991  
1000-500MB THKN (DAM) --- VALID 12Z MON 22 APR 1991



RAFS 36-HOUR FORECAST

Fig 13. U.S. operational regional model (NGM) forecasts of sea level pressure (mb, solid lines) and 1000-500 mb thickness (dam, dashed lines), verifying at 1200 UTC 22 April 1991. 48-h forecast is shown as the upper panel, and 36-h forecast as the lower panel.

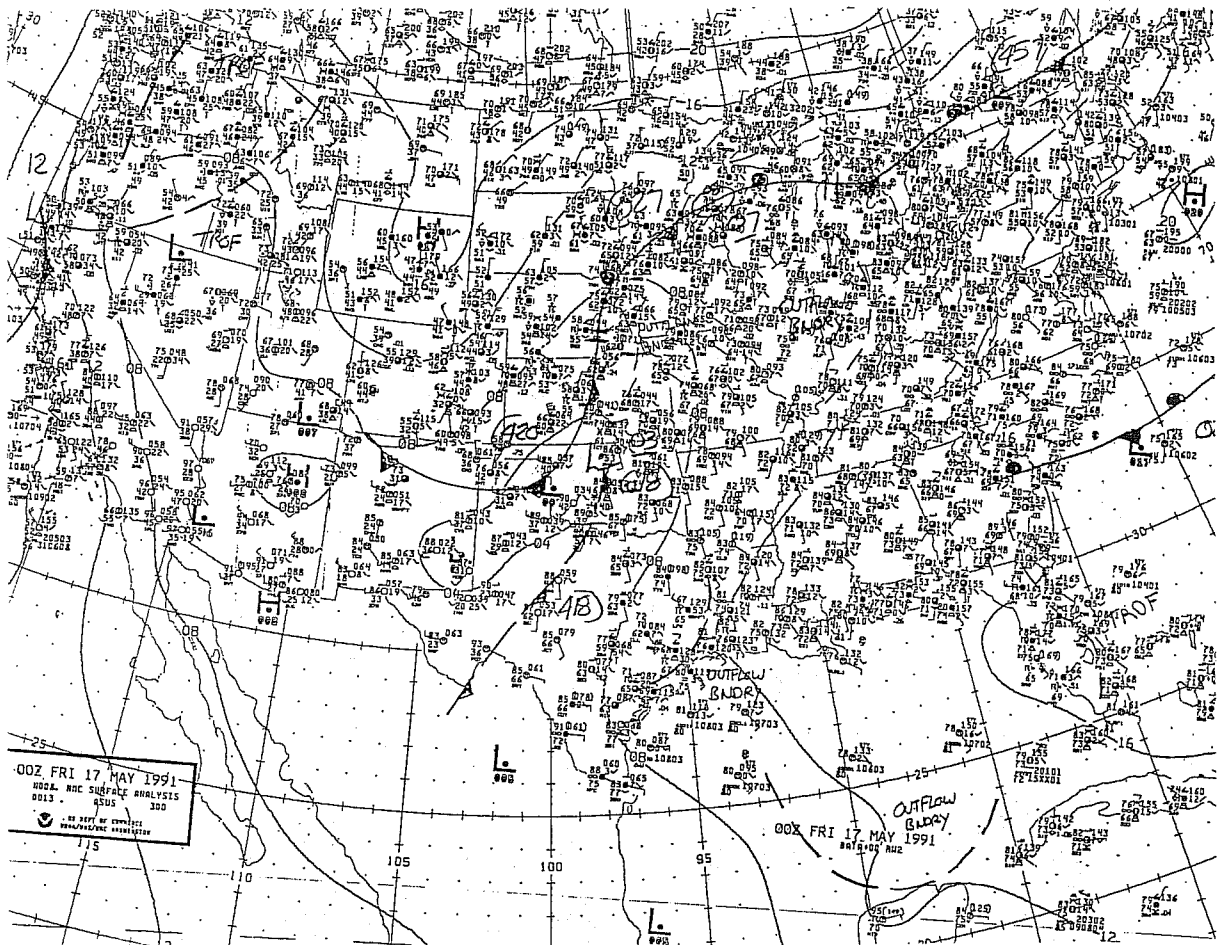


Fig. 14. A section of the NMC surface analysis for 0000 UTC 17 May 1991.

Montana and North Dakota, coming behind the main trough to the southeast and east of it. This ridge axis runs from Montana into western and central Wyoming in the sigma forecast, in contrast to its running from the Montana-North Dakota border into eastern Wyoming in the eta forecast. This latter position is in agreement with the verification in Fig. 14; yet both are too intense.

In Fig. 16 the NGM forecast is shown starting with the same initial conditions and verifying at the same time. The center of the low pressure area over Oklahoma is somewhat too deep in the NGM integration and the ridge behind it is even slower than in the sigma mode integration of Fig. 15. To the northeast of the ridge in northern Manitoba the center of the high in both the NGM forecast and in the sigma mode forecast of Fig. 15 is 1032 mb. The NMC analysis has this center at 1030 mb and the eta mode forecast at 1029 mb.

Noise. A major cause of the overabundance of sea level pressure centers on the six Eta Model maps shown is the reduction to sea level used, based on the lowest layer temperatures. When



# Mesinger, Fedor: Vertical Discretization and Coordinate Systems

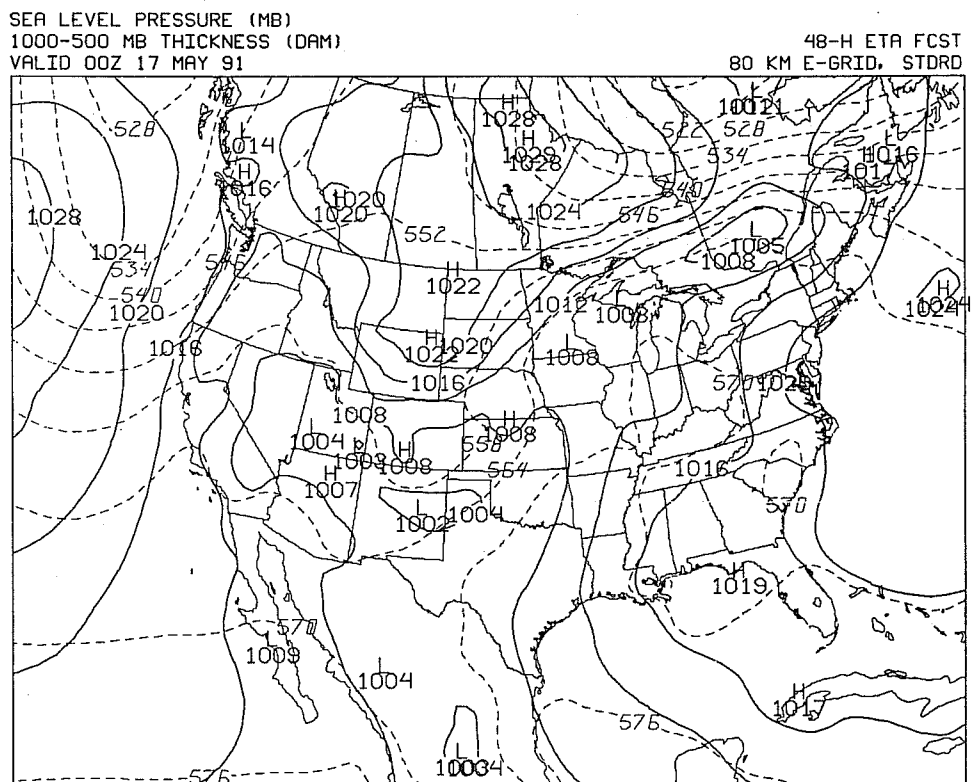
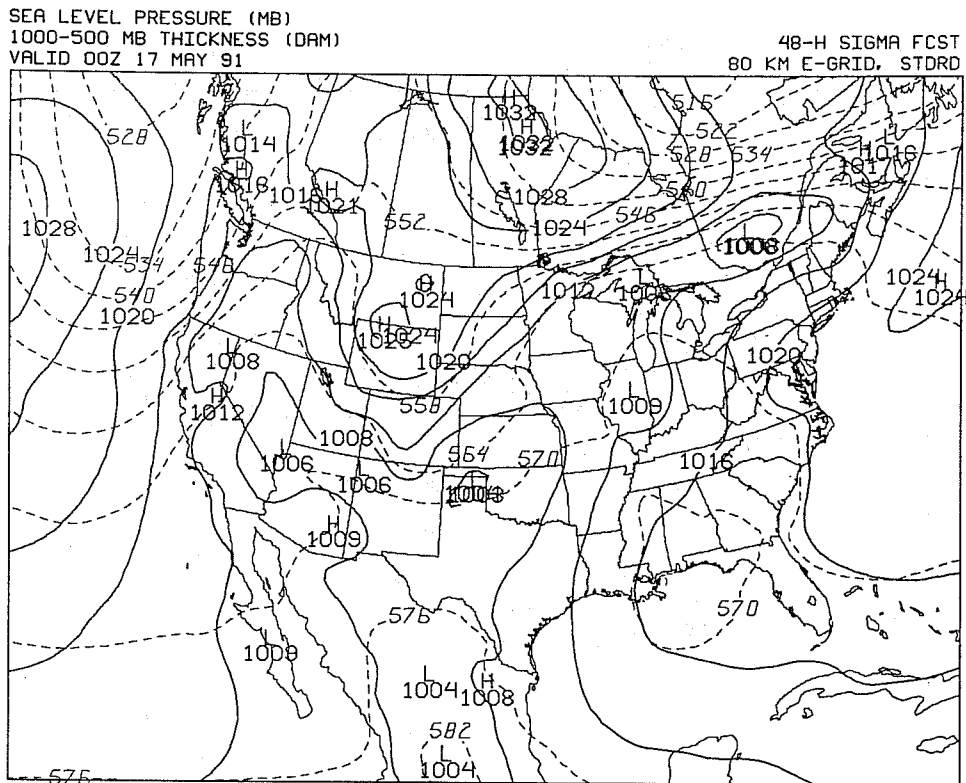


Fig 15. As in Fig. 8 except for verifying at 0000 UTC 17 May 1991.

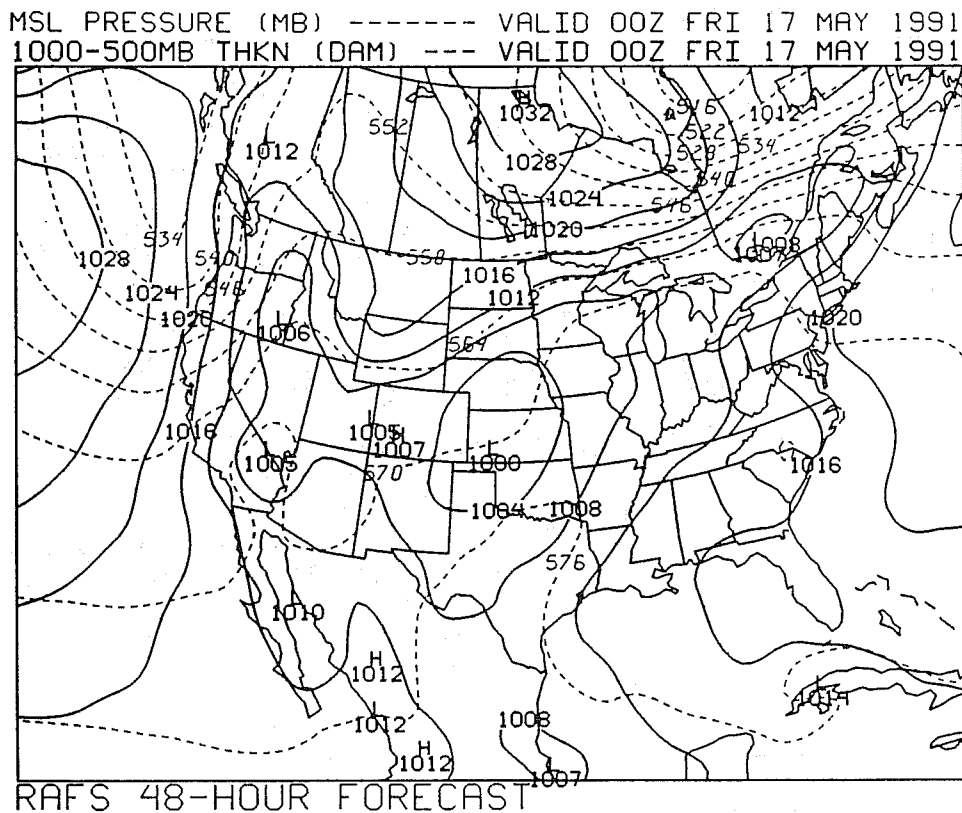


Fig. 16. U.S. operational regional model (NGM) 48-h forecast of sea level pressure (mb, solid lines) and 1000-500 mb thickness (dam, dashed lines), verifying at 0000 UTC 17 May 1991.

the standard Eta Model reduction based on horizontally interpolated virtual temperatures is used the number of centers is greatly reduced.

The number of pressure centers printed thus gives one measure of the noisiness of integrations as some of the centers are not realistic but are due to the noisiness of the lowest layer temperatures. One may therefore wish to compare the number of centers in the pairs of integrations shown. There are two more centers in the sigma map of Fig. 8, and four more centers in the sigma map of Fig. 12 than in the corresponding eta maps. The number of centers on the two maps in Fig. 15 is the same. Overall, of the 12 pairs of maps we had produced for the three integrations there were a total of 18 more centers on the sigma maps. Comparing individual pairs of maps, the sigma maps had more centers eight times, the eta maps twice, and the number of centers was the same twice.

This, of course, is only one indication of the noisiness. In the early eta/sigma integrations the sigma mode noisiness near the surface was not nearly as prominent as it was near the tropospheric jet stream level.

Summary and plans. Of the results shown perhaps the consistency of the sigma integration errors of the two different sigma models is the result deserving most attention. The errors of the two sigma models either had an almost identical pattern (the last two cases) or seemed to have the same basic cause (the February 89 case). We feel that this underscores the importance of the issues involved as it indicates that errors are indeed inherently due to the sigma representation rather than due to the specifics of the numerical scheme of a sigma system model.

We are planning to gather more quantitative information on the sigma vs. eta errors. We are at the same time in the process of assessing the need for thin layers or requirements due to the lack thereof over elevated terrain by looking at the performance and efficiency of various schemes for calculation of surface fluxes. One must remember, though, that sloping thin layers are not without problems of their own as they lead to a violation of the hydrostatic consistency condition of standard finite-difference schemes for calculation of the pressure gradient force (Janjić, 1977; Mesinger, 1982).

## 5. CONCLUSIONS

With such a diverse variety of arguments at play and some of them in conflict with others, different decisions by various modelers and modeling groups are unavoidable and probably welcome. Awareness of the issues involved presumably leading to appropriate verification efforts is about as much as one can do in getting guidance from the theoretical and conceptual considerations summarized in this lecture. "The proof of the pudding is in the eating" are as appropriate words of wisdom in the vertical discretization area as any of the specific arguments presented.

The prospect of being able to use ever higher resolutions for some time to come is an important factor. Recall that various errors discussed are very different in the sense that some can obviously be reduced or eliminated with an increase in resolution while others require judicious decisions in terms of the vertical vs. horizontal resolution. Those where an increase in resolution may not be of any help are the most deserving of our attention.

Acknowledgment. In addition to participating in the experiments I have reported on in Section 4.2 Tom Black of the National Meteorological Center has read the manuscript and has made numerous suggestions which have much improved the readability of the text.

## REFERENCES

- Achtemeier, G. L., 1991: Reducing hydrostatic truncation error in a mesobeta boundary layer model. *Mon. Wea. Rev.*, 119, 223-229.
- Arakawa, A., 1988: Finite-difference methods in climate modeling. *Physically-Based Modelling and Simulation of Climate and Climatic Change, Part I*, M. E. Schlesinger, Ed., Kluwer Academic, 79-168.

Arakawa, A., and V. R. Lamb, 1977: Computational design of the basic dynamical processes of the UCLA general circulation model. *Methods in Computational Physics*, Vol. 17, J. Chang, Ed., Academic Press, 173-265.

Arakawa, A., and S. Moorthi, 1988: Baroclinic instability in vertically discrete systems. *J. Atmos. Sci.*, **45**, 1688-1707.

Benjamin, S. G., T. L. Smith, P. A. Miller, D. Kim, T. W. Schlatter and R. Bleck, 1991: Recent improvements in the MAPS isentropic-sigma data assimilation system. Preprints, Ninth Conf. Numerical Weather Prediction, Denver, CO, Amer. Meteor. Soc., 118-121. [Boston, MA 02108.]

Black, T. L., 1987: A comparison of key forecast variables derived from isentropic and sigma coordinate regional models. *Mon. Wea. Rev.*, **115**, 3097-3114.

Bleck, R., 1984: An isentropic coordinate model suitable for lee cyclogenesis simulation. *Riv. Meteor. Aeronautica*, **44**, 189-194.

Carpenter, R. L., Jr., K. K. Droegemeier, P. W. Woodward and C. E. Hane, 1990: Application of the piecewise parabolic method (PPM) to meteorological modeling. *Mon. Wea. Rev.*, **118**, 586-612.

Carroll, J. J., L. R-Mendez-Nunez, and S. Tanrikulu, 1987: Accurate pressure gradient calculations in hydrostatic atmospheric models. *Boundary-Layer Meteor.*, **41**, 149-169.

ECMWF, 1984: Numerical Methods for Weather Prediction, Vols. 1 and 2. Seminar 1983, ECMWF, Shinfield Park, Reading, U.K., 290+300 pp.

Eliassen, A., and E. Raustein, 1968: A numerical integration experiment with a model atmosphere based on isentropic coordinates. *Meteor. Ann.*, **5**, 45-63.

Haney, R. L., 1991: On the pressure gradient force over steep topography in sigma coordinate ocean models. *J. Phys. Oceanogr.*, **21**, 610-619.

Hoke, J. E., N. A. Phillips, G. J. DiMego, J. J. Tuccillo and J. G. Sela, 1989: The regional analysis and forecast system of the National Meteorological Center. *Wea. Forecasting*, **4**, 323-334.

Hsu, Y.-J., and A. Arakawa, 1990: Numerical modeling of the atmosphere with an isentropic vertical coordinate. *Mon. Wea. Rev.*, **118**, 1933-1959.

Janjić, Z. I., 1977: Pressure gradient force and advection scheme used for forecasting with steep and small scale topography. *Contributions to Atmospheric Physics*, **50**, 186-199.

Janjić, Z. I., 1990: The step-mountain coordinate: physical package. *Mon. Wea. Rev.*, **118**, 1429-1443.

Kanamitsu, M., 1989: Description of the NMC global data assimilation and forecast system. *Wea. Forecasting*, **4**, 335-342.

Konor, C. S., K. M. Hines, C. R. Mechoso and A. Arakawa, 1991: Simulation of frontogenesis with sigma and isentropic vertical-coordinate models. Preprints, Ninth Conf. Numerical Weather Prediction, Denver, CO, Amer. Meteor. Soc., 305-308. [Boston, MA 02108.]

- Leslie, L. M., G. A. Mills, L. W. Logan, D. J. Gauntlett, G. A. Kelly, M. J. Manton, J. L. McGregor and J. M. Sardie, 1985: A high resolution primitive equations NWP model for operations and research. *Aust. Meteor. Mag.*, **33**, 11-35.
- Leslie, L. M., and R. J. Purser, 1991a: High-order numerics in an unstaggered three-dimensional time-split semi-Lagrangian forecast model. *Mon. Wea. Rev.*, **119**, 1612-1623.
- Leslie, L. M., and R. J. Purser, 1991b: A comparative study of the performance of various vertical discretization schemes. *Subm. to Meteor. Atmos. Phys.*
- Lindzen, R. S., and M. Fox-Rabinovitz, 1989: Consistent vertical and horizontal resolution. *Mon. Wea. Rev.*, **117**, 2575-2583.
- Lorenz, E. N., 1960: Energy and numerical weather prediction. *Tellus*, **12**, 364-373.
- Mattocks, C., and R. Bleck, 1986: Jet streak dynamics and geostrophic adjustment processes during the initial stages of lee cyclogenesis. *Mon. Wea. Rev.*, **114**, 2023-2056.
- Mesinger, F., 1982: On the convergence and error problems of the calculation of the pressure gradient force in sigma coordinate models. *Geophys. Astrophys. Fluid. Dyn.*, **19**, 105-117.
- Mesinger, F., 1984: A blocking technique for representation of mountains in atmospheric models. *Riv. Meteor. Aeronautica*, **44**, 195-202.
- Mesinger, F., 1990: "Horizontal" pressure reduction to sea level. In: Preprints, 21. internationale Tagung für alpine Meteorologie, 17.-21. September 1990, Engelberg, Schweiz. Schweizerische meteorologische Anstalt, Krähbühlstrasse 58, CH-8044 Zürich, Switzerland, 31-35.
- Mesinger, F., and Z. I. Janjić, 1985: Problems and numerical methods of the incorporation of mountains in atmospheric models. *Large-scale Computations in Fluid Mechanics, Part 2. Lect. Appl. Math.*, Vol. 22, Amer. Math. Soc., 81-120.
- Mesinger, F., and Z. I. Janjić, 1987: Numerical techniques for the representation of mountains in atmospheric models. *Observation, Theory and Modelling of Orographic Effects, Seminar/workshop 1986, Vol. 2, ECMWF, Shinfield Park, Reading, U.K.*, 29-80.
- Mesinger, F., and Z. I. Janjić, 1990: Numerical methods for the primitive equations (space). *10 Years of Medium-Range Weather Forecasting, Seminar 1989, Vol. 1, ECMWF, Shinfield Park, Reading, U.K.*, 205-251.
- Mesinger, F., T. L. Black and Z. I. Janjić, 1988a: Sigma system contribution to systematic errors in models of the atmosphere. In: *Workshop on Systematic Errors in Models of the Atmosphere, Toronto, 19-23 September 1988, CAS/JSC Working Group on Numerical Experimentation Rept. No. 12, WMO, Geneva*, 253-263.
- Mesinger, F., Z. I. Janjić, S. Ničković, D. Gavrilov and D. G. Deaven, 1988b: The step-mountain coordinate: model description and performance for cases of Alpine lee cyclogenesis and for a case of Appalachian redevelopment. *Mon. Wea. Rev.*, **116**, 1493-1518.

Pecnick, M. J., and D. Keyser, 1989: The effect of spatial resolution on the simulation of upper-tropospheric frontogenesis using a sigma-coordinate primitive-equation model. *Meteor. Atmos. Phys.*, **40**, 137-149.

Persson, P. O. G., and T. T. Warner, 1991: Model generation of spurious gravity waves due to inconsistency of the vertical and horizontal resolution. *Mon. Wea. Rev.*, **119**, 917-935.  
Phillips, N. A., 1957: A coordinate system having some special advantages for numerical forecasting. *J. Meteor.*, **14**, 184-185.

Pierce, R. B., D. R. Johnson, F. M. Reames, T. H. Zapotocny and B. J. Wolf, 1991: Numerical investigations with a hybrid isentropic-sigma model. Part I: Normal mode characteristics. *J. Atmos. Sci.*, (in press).

Purser, R. J., and L. M. Leslie, 1991: A comparative study of the performance of various vertical discretization schemes. Preprints, Ninth Conf. Numerical Weather Prediction, Denver, CO, Amer. Meteor. Soc., 313-315. [Boston, MA 02108.]

Sela, J. G., 1982: The NMC Spectral Model. NOAA Tech. Rep. NWS 30, National Weather Service, Silver Spring, MD., 36 pp.

Simmons, A. J., and D. M. Burridge, 1981: An energy and angular-momentum conserving vertical finite-difference scheme and hybrid vertical coordinates. *Mon. Wea. Rev.*, **109**, 758-766.

Steppeler, J., 1989: A three dimensional global weather prediction model using a finite element scheme for vertical discretization. *Int. J. Numer. Meth. Engin.*, **106**, 439-447.

Tafferer, A., and J. Egger, 1990: Test of theories of lee cyclogenesis: ALPEX cases. *J. Atmos. Sci.*, **47**, 2417-2428.

Thompson, W. T., and S. D. Burk, 1991: An investigation of an arctic front with a vertically nested mesoscale model. *Mon. Wea. Rev.*, **119**, 233-261.

Tokioka, T., 1978: Some consideration on vertical differencing. *J. Meteor. Soc. Japan*, **56**, 89-111.